Resonant $dt\mu$ formation in condensed hydrogen isotopes

Andrzej Adamczak*
Institute of Nuclear Physics, Polish Academy of Sciences, Radzikowskiego 152, PL-31342 Kraków, Poland

Mark P. Faifman†
Russian Research Center Kurchatov Institute, Kurchatov Square 1, RU-123182 Moscow, Russia
(Received 15 March 2005; revised manuscript received 9 August 2005; published 3 November 2005)

Resonant formation of the muonic molecule $dt\mu$ in $t\mu$ atom collision with condensed H-D-T targets is considered. A specific resonance correlation function, which is a generalization of the Van Hove single-particle correlation function, is introduced to calculate the resonant-formation rate in such targets. This function is derived in the case of a polycrystalline harmonic solid. Also, a general asymptotic form of the resonance correlation function for high momentum transfers is found, which is valid for any solid or dense-fluid hydrogen-isotope target. Numerical calculations of the rates are performed for solid hydrogen isotopes at zero pressure, using the isotropic Debye model of a solid. It is shown that condensed-matter effects in resonant formation are strong, which explains some unexpected experimental results. In particular, the resonance profiles are affected by large zero-point vibrations of the hydrogen-isotope molecules bound in the considered crystals, even for high ($\sim$1 eV) collision energies. This is important for explaining the time-of-flight measurements of the $dt\mu$-formation rate, carried out at TRIUMF. The calculated mean values of the formation rate in solid D-T targets, for fixed target temperatures and steady-state conditions, are in good agreement with the PSI and RIKEN-RAL experiments.

DOI: 10.1103/PhysRevA.72.052501 PACS number(s): 36.10.Dr, 34.50.−s

I. INTRODUCTION

A theoretical study of the resonant formation of the muonic molecular ion $dt\mu$ in condensed hydrogen-isotope targets is the main subject of this paper. Formation of $dt\mu$ in collision of a $t\mu$ atom with a hydrogen-isotope molecule is a key process of muon-catalyzed fusion (μCF) in a D-T mixture. This phenomenon has attracted particular interest because one muon can catalyze more than 100 fusions [1–4] according to the reaction

$$dt\mu \rightarrow {}^4\mathrm{He} + n + \mu^- + 17.6\ \mathrm{MeV}.$$

Investigation of the μCF cycle in hydrogen-isotope targets is also important for studies of various phenomena in atomic, molecular, and nuclear physics (see reviews [5–7]).

Resonant $dt\mu$ formation is due to the presence of a loosely bound state of $dt\mu$ [1] with the rotational quantum number $J=1$, the vibrational quantum number $v=1$, and the binding energy $\varepsilon_{Jv=11}\approx -0.63$ eV. Theoretical methods for calculating the resonant-formation rates have been developed over many years (see, e.g., Refs. [8–16]). These methods, taking into account resonant formation in $t\mu$ collisions with one or several molecules, show good agreement with the experimental data for dilute gaseous targets. However, such a theory is unable to explain various phenomena found in experiments with dense fluid and solid hydrogen-isotope targets. This concerns a nonlinear dependence of the formation rate on the target density [4,17], puzzling temperature effects [18], and the resonance profiles determined by the time-of-flight experiments [19–22]. Therefore, it is necessary to consider an influence of many-body effects on muonic-molecule formation. In particular, different collective phenomena can significantly change this process, which one can expect knowing their role in resonant neutron absorption by nuclei bound in condensed matter [23,24].

Condensed-matter effects in resonant neutron absorption can be expressed in terms of the incoherent correlation function [24], which was introduced by Van Hove [25] for the description of incoherent neutron scattering. This function depends on the energy and momentum transfer to a given target and on the target properties. Application of the classical correlation function to resonant absorption phenomena is possible only if a change of the target-particle mass due to absorption can be neglected. This is a good approximation for neutron absorption by much heavier nuclei, at any collision energy.

It is also possible to adapt the Van Hove formalism to resonant muonic-molecule formation in a condensed target. However, the mass of an impinging muonic atom is comparable with that of a hydrogen-isotope molecule. Therefore, application of the usual correlation function to such a process gives good results only at lowest collision energies ($\lesssim$10 meV), when the molecule is strongly bound in a target during formation process.

A first estimation of the low-energy $dt\mu$-formation rates in solid molecular deuterium, using the standard correlation-function formalism, was performed by Fukushima [26]. He performed an *ab initio* calculation of lattice dynamics to determine the correlation function and demonstrated an important role of phonon processes in resonant $dt\mu$ formation. His calculation was limited to high target pressures ($\sim$10 kbar), where molecular hydrogen-isotope solids become classical

*Electronic address: andrzej.adamczak@ifj.edu.pl
†Electronic address: mark@rogova.ru

crystals. However, in μCF experiments, only zero or low pressure ($\ll$10 kbar) have been applied. In such conditions, solid-hydrogen targets are quantum crystals characterized by large amplitudes of zero-point vibration of hydrogen molecules in lattices. As a result, a special approach is necessary to solve lattice dynamics [27,28]. Owing to this fact and to a rough estimation of the transition-matrix elements for $dt\mu$ formation, the results of Ref. [26] are about 5 times greater than the rates determined in experiments [2,4]. Moreover, the temperature dependence of the calculated formation rate, for a D_2 molecule bound in solid D-T, is opposite to what has been recently seen in the RIKEN-RAL experiment [18].

The standard correlation function, which had been rigorously derived for a perfect gas, for a harmonic lattice, and for any system in the high-energy limit [25], was then applied for the description of resonant $dd\mu$-formation in condensed deuterium at lowest energies [29]. The correlation function for solid polycrystalline D_2 was evaluated using the Debye model of an isotropic solid. The model parameters, such as the Debye temperature and the lattice constants, were taken from the available data including quantum-crystal effects [27,28]. Therefore, the results of Ref. [29] are valid also for zero- or low-pressure solid deuterium. Since the $dd\mu$ resonances for a free D_2 molecule are very narrow, their profiles were assumed to have the δ-function shape. In Ref. [29] also a rough estimate of the $dd\mu$-formation rate for high energies was given. This estimate did not take into account a change of the target mass. However, such an approach is sufficient for the description of muon-catalyzed *dd* fusion in solid deuterium, when the role of low-energy resonances is dominant due to very fast $d\mu$ deceleration to energies below 10 meV. In particular, the time spectra of *dd*-fusion products calculated in Ref. [29] are in good agreement with the data taken at TRIUMF [30].

The explanation of experiments concerning resonant $dt\mu$ formation in condensed hydrogen isotopes requires a significant extension of the theoretical framework developed in Ref. [29] for $dd\mu$ formation. First, profiles of the $dt\mu$ resonances for an isolated target molecule are much wider than those for the $dd\mu$ case. Thus, they are described by the Breit-Wigner function with considerable width [9,31]. Second, the time-of-flight experiments using energetic ($\sim$1 eV) beams of $t\mu$ atoms [20–22] require knowledge of accurate formation rates at energies much greater than 10 meV. In this case, a change of the target-particle mass, connected with the replacement of a hydrogen-isotope molecule by a much heavier muonic-molecular complex with the $dt\mu$ ion inside, cannot be neglected. In particular, inclusion of this change gives the correct recoiling mass in the limit of high $t\mu$ energy. This is why the $dt\mu$-formation rate cannot be expressed in terms of the standard correlation function. As we show below, the Van Hove formalism can, however, be applied to higher-energy $dt\mu$ formation if a special resonance correlation function that includes the discussed mass change is introduced. This function is much more complicated than the classical correlation function used in Refs. [24,26,29]. However, we have found solutions for some important cases.

In Sec. II, a brief description of resonant $dt\mu$ formation in an isolated hydrogen-isotope molecule and some basic formulas are given. A method for calculating the $dt\mu$-formation rates in condensed targets, for the Breit-Wigner profiles and for any collision energy, is presented in Sec. III. In particular, the resonance correlation function is defined and then derived in the case of harmonic polycrystalline hydrogen isotopes, for low and intermediate collision energies. At high energies, this function takes a general simple form, which is valid for any hydrogen-isotope target—solid, liquid, or gaseous. Assuming zero resonance widths and neglecting the mass change of the target molecule in the formation process, the rates derived below coincide with the formulas for $dd\mu$ formation obtained in Ref. [29]. Some results of numerical calculations for $dt\mu$ formation in low-pressure hydrogen-isotope solids are presented in Sec. IV. A full set of energy-dependent transition-matrix elements has been calculated for free molecules HD, D_2, and DT, which establishes the input for estimating the $dt\mu$-formation rates in condensed hydrogen isotopes. The $dt\mu$-formation rates for some typical solid targets are shown as functions of the $t\mu$ kinetic energy and target temperature. In particular, contributions from different resonances to the total formation rates and influence of the ortho-D_2 and para-D_2 concentration in a target on the formation rates are considered. A comparison of the calculated mean rates with experimental results is performed.

II. RESONANT FORMATION IN A FREE MOLECULE

First we consider resonant formation of $dt\mu$ in the following reaction:

$$(t\mu)_F + (\mathrm{D}C)^I_{\nu_i K_i} \rightarrow [(dt\mu)^S_{Jv} cee]_{\nu_f K_f},$$

$$C = \mathrm{H,D,\ or\ T} \quad \text{and} \quad c = p,d,\ \text{or}\ t,$$

where DC is a free molecule in the initial rotational-vibrational state $(\nu_i K_i)$ with total nuclear spin **I**. This spin is taken into account for DC=D_2. The $t\mu$ atom has total spin **F** and a center-of-mass (c.m.) kinetic energy ε. The molecular complex $[(dt\mu)cee]$ is created in the rotational-vibrational state $(\nu_f K_f)$, and the molecular ion $dt\mu$, which plays the role of a heavy nucleus of the complex, has total spin **S**. This process takes place due to the presence of a loosely bound state of $dt\mu$ with rotational number $J=1$ and vibrational number $v=1$. The binding energy $|\varepsilon_{Jv=11}| \approx 0.63$ eV released in the above reaction is transferred to rotational-vibrational degrees of freedom of the created molecular complex $[(dt\mu)cee]$. The resonance condition is fulfilled when ε takes a specific value ε^0_{if}. This is the so-called Vesman's mechanism of muonic-molecule formation, introduced in Ref. [8] for the $dd\mu$ case. In the Vesman model, the resonance width is infinitely small, so that the resonant-formation rate has the Dirac delta function profile.

In the case of resonant $dd\mu$ formation, the rates calculated using Vesman's model agree very well with experiments [32,33]. On the other hand, the assumption of the δ-function profile for $dt\mu$ resonances has led to inconsistency with experiments in gaseous D-T targets performed at low temperatures [3,4,34,35]. The measured rates are much greater than the theoretical predictions based on the Vesman model. It has been pointed out by Petrov [9] that the $dt\mu$ resonances

should have broader Breit-Wigner profiles, owing to a finite lifetime of the complex. At low temperatures, this leads to significant contributions to the formation rates [36] from the subthreshold resonances $\varepsilon_{if}^0<0$. Thus, in a general free-molecule case, the resonance-formation rate takes the following form (in atomic units $e=\hbar=m_e=1$) [9,11]:

$$\lambda^{SF}_{\nu_i K_i,\nu_f K_f} = N_{\rm mol} B_{if} |V_{if}(\varepsilon)|^2 \frac{\Gamma_S}{(\varepsilon-\varepsilon_{if}^0)^2+\frac{1}{4}\Gamma_S^2}, \qquad (1)$$

where $N_{\rm mol}$ is the number density of hydrogen-isotope molecules in the target. The natural width Γ_S of a given resonance is equal to the sum of the effective fusion rate λ_f and the total rate $\lambda^S_{\rm bck}$ of back decay of the complex [13,37,38]:

$$\Gamma_S = \lambda_f + \lambda^S_{\rm bck}. \qquad (2)$$

The transition-matrix element $V_{if}(\varepsilon)$ and resonance energy ε_{if}^0 are defined in Ref. [13]. The factor B_{if} is given as

$$B_{if} = \frac{2S+1}{3(2F+1)} q_d,$$

where $q_d=1$ for asymmetric molecules DC and $q_d=2$ for D_2.

Equation (1) was employed in Refs. [16,39] for the calculation of the $dt\mu$-formation rate in a diluted D_2 gas, which led to agreement with the experimental data [35].

III. RESONANT FORMATION IN A CONDENSED TARGET

A. Method of calculation

When the formation of a muonic molecule takes place in a dense target, it is necessary to take into account interactions of an impinging muonic atom with more than one molecule. In particular, energy transfer to many molecules is possible, which results in a quasiresonant character of the formation process. A quasiresonant mechanism of $dt\mu$ formation was first considered in Ref. [10], for triple collisions $t\mu+D_2+D_2$, in order to explain the nonlinear dependence of the $dt\mu$-formation rate on the target density. In this case, formation is possible even if the resonance condition is not strictly fulfilled, because the energy excess in the $t\mu+D_2$ system is transferred to a neighbor molecule. The three-body reactions and broadening of the resonance profiles were then discussed in Refs. [12,15,31,36]. If the target is condensed, it is indispensable to also take into account the influence of collective molecular motions on quasiresonant formation, which was shown in Ref. [29] for the $dd\mu$ case. A scheme of quasiresonant $dt\mu$ formation in $t\mu$ collision with a condensed D_2 target at kinetic energy ε is presented in Fig. 1. Energy balance, including energy transfer ω to a target, is shown for a subthreshold resonance corresponding to the vibrational transition $\nu_i=0\rightarrow\nu_f=2$. Since the target molecule and the complex $[(dt\mu)dee]$ are bound, the corresponding resonance energy ε_{if} is different from the "free" resonant energy ε_{if}^0, characterized by the same set of quantum numbers.

Reasoning similar to that presented in Ref. [29] leads to the following formula for the $dt\mu$-formation rate in a condensed target:

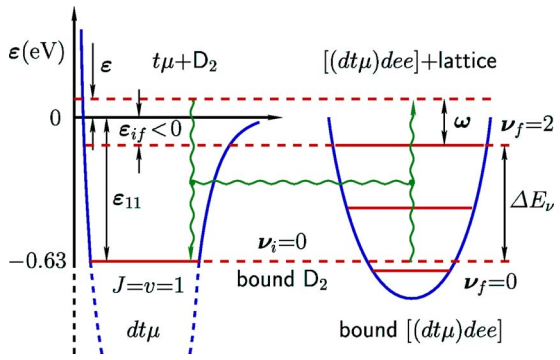

FIG. 1. (Color online) Energy balance for quasiresonant formation of $dt\mu$ in a D_2 molecule bound in a condensed target.

$$\lambda^{SF}_{\nu_i K_i,\nu_f K_f} = N_{\rm mol} B_{if} |\mathcal{A}_{i0,fn}|^2 \frac{\Gamma_S}{(\varepsilon+E_0-\varepsilon_{if}^0-\tilde{E}_n)^2+\frac{1}{4}\Gamma_S^2}, \qquad (3)$$

where the matrix element $\mathcal{A}_{i0,fn}$ is expressed by the energy-dependent matrix element $V_{if}(\varepsilon)$ calculated for a free molecule,

$$\mathcal{A}_{i0,fn} = \langle\tilde{n}|\exp(i\mathbf{k}\cdot\mathbf{R}_l)|0\rangle V_{if}(\varepsilon). \qquad (4)$$

The eigenvalues of the initial $\mathcal{H}$ and final $\tilde{\mathcal{H}}$ Hamiltonians of the target, corresponding to the eigenstates $|0\rangle$ and $|\tilde{n}\rangle$, are denoted by E_0 and $\tilde{E}_n$, respectively. The vector $\mathbf{k}$ stands for the initial momentum of the $t\mu$ atom. Resonant $dt\mu$ formation takes place in $t\mu$ collision with the lth molecule DC. The vector $\mathbf{R}_l$ shows the position of its mass center in the target frame (see Fig. 2). A change of the target Hamiltonian $\Delta\mathcal{H}\equiv\mathcal{H}-\tilde{\mathcal{H}}$ is due to replacement of molecule DC by the complex $[(dt\mu)cee]$. It can be shown that $\Delta\mathcal{H}$ is expressed by the molecular-kinetic-energy operator [29]

$$\Delta\mathcal{H} = -\alpha\frac{1}{2M_{\rm DC}}\nabla^2_{R_l}, \quad \alpha\equiv 1-\frac{M_{\rm DC}}{M_{\rm cplx}} \lesssim \frac{1}{2}, \qquad (5)$$

where $M_{\rm cplx}$ is the mass of the complex and $M_{\rm DC}$ is the mass of the molecule DC. A small contribution to $\Delta\mathcal{H}$ due to

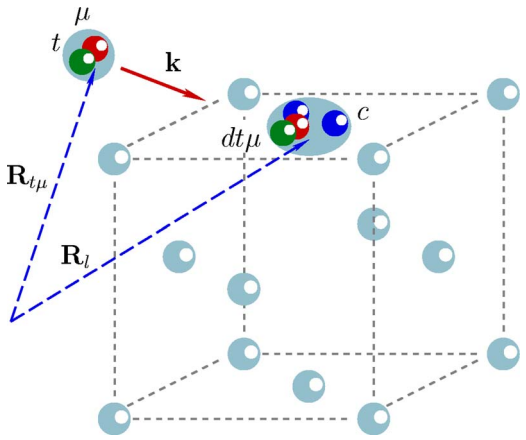

FIG. 2. (Color online) Quasiresonant $dt\mu$ formation in $t\mu$-atom collision with a bound molecule DC.

replacement of the DC center of mass by that of the complex is neglected here.

Averaging the rate (3) over the distribution ρ_{n_0} of the initial target states at a given temperature T and summing over the final target states leads to

$$\lambda^{SF}_{\nu_i K_i,\nu_f K_f} = N_{\mathrm{mol}} B_{if} |V_{if}|^2 \Gamma_S \times \sum_{n,n_0} \rho_{n_0} \frac{|\langle \tilde{n}|\exp(i\mathbf{k}\cdot\mathbf{R}_l)|0\rangle|^2}{(\varepsilon + E_0 - \varepsilon^0_{if} - \tilde{E}_n)^2 + \frac{1}{4}\Gamma_S^2}.$$

The above equation can be written down in integral form

$$\lambda^{SF}_{\nu_i K_i,\nu_f K_f} = N_{\mathrm{mol}} B_{if} |V_{if}|^2 \Gamma_S \sum_{n,n_0} \rho_{n_0} |\langle \tilde{n}|\exp(i\mathbf{k}\cdot\mathbf{R}_l)|0\rangle|^2 \times \int_{-\infty}^{\infty} dE \frac{\delta(E - \tilde{E}_n + E_0)}{(\varepsilon - \varepsilon^0_{if} - E)^2 + \frac{1}{4}\Gamma_S^2}.$$

Now we use a time variable t to eliminate the δ function in the above equation and then we introduce time-dependent operators, which are well-known in scattering theory [40,41]. Applying the Fourier expansion of the δ function one obtains

$$\lambda^{SF}_{\nu_i K_i,\nu_f K_f} = \frac{1}{2\pi} N_{\mathrm{mol}} B_{if} |V_{if}|^2 \Gamma_S \int_{-\infty}^{\infty} dt \sum_{n,n_0} \rho_{n_0} |\langle \tilde{n}| \times \exp(i\mathbf{k}\cdot\mathbf{R}_l)|0\rangle|^2 \exp[it(\tilde{E}_n - E_0)] \times \int_{-\infty}^{\infty} dE \frac{\exp(-iEt)}{(\varepsilon - \varepsilon^0_{if} - E)^2 + \frac{1}{4}\Gamma_S^2},$$

which, after integration over E, gives

$$\lambda^{SF}_{\nu_i K_i,\nu_f K_f} = N_{\mathrm{mol}} B_{if} |V_{if}|^2 \int_{-\infty}^{\infty} dt \exp\left[-it(\varepsilon - \varepsilon^0_{if}) - \frac{1}{2}\Gamma_S |t| \right] \sum_{n,n_0} \rho_{n_0} \langle 0|\exp(-i\mathbf{k}\cdot\mathbf{R}_l)|\tilde{n}\rangle \times \langle \tilde{n}|\exp(it\tilde{E}_n)\exp(i\mathbf{k}\cdot\mathbf{R}_l)\exp(-itE_0)|0\rangle. \quad (6)$$

The matrix element in Eq. (6) can be written as follows:

$$\langle \tilde{n}|\exp(it\tilde{E}_n)\exp(i\mathbf{k}\cdot\mathbf{R}_l)\exp(-itE_0)|0\rangle = \langle \tilde{n}|\exp(it\widetilde{\mathcal{H}})\exp(i\mathbf{k}\cdot\mathbf{R}_l)\exp(-it\mathcal{H})|0\rangle = \langle \tilde{n}| \times \exp(it\widetilde{\mathcal{H}})\exp(-it\mathcal{H})\exp(it\mathcal{H})\exp(i\mathbf{k}\cdot\mathbf{R}_l)\exp(-it\mathcal{H}) \times |0\rangle = \langle \tilde{n}|\exp(it\widetilde{\mathcal{H}})\exp(-it\mathcal{H})\exp[i\mathbf{k}\cdot\mathbf{R}_l(t)]|0\rangle,$$

where $\mathbf{R}_l(t)$ denotes the Heisenberg operator,

$$\mathbf{R}_l(t) = \exp(it\mathcal{H})\mathbf{R}_l \exp(-it\mathcal{H}),$$

defined for all l and t.

Employing the identity $\Sigma_n |\tilde{n}\rangle\langle\tilde{n}| = 1$ in Eq. (6) we obtain a general expression for the quasiresonant formation rate:

$$\lambda^{SF}_{\nu_i K_i,\nu_f K_f} = 2\pi N_{\mathrm{mol}} B_{if} |V_{if}|^2 \mathcal{S}_{\mathrm{res}}(\mathbf{k}, \varepsilon - \varepsilon^0_{if}), \quad (7)$$

where $\mathcal{S}_{\mathrm{res}}$ is the *resonance response function* defined as

$$\mathcal{S}_{\mathrm{res}}(\mathbf{k}, \varepsilon - \varepsilon^0_{if}) \equiv \frac{1}{2\pi} \int_{-\infty}^{\infty} dt \exp\left[-it(\varepsilon - \varepsilon^0_{if}) - \frac{1}{2}\Gamma_S |t| \right] \times \mathcal{Y}_{\mathrm{res}}(\mathbf{k}, t). \quad (8)$$

Function $\mathcal{Y}_{\mathrm{res}}(\mathbf{k}, t)$ denotes here the following *resonance correlation function*:

$$\mathcal{Y}_{\mathrm{res}}(\mathbf{k}, t) \equiv \langle \exp[-i\mathbf{k}\cdot\mathbf{R}_l(0)]\exp(it\widetilde{\mathcal{H}}) \times \exp(-it\mathcal{H})\exp[i\mathbf{k}\cdot\mathbf{R}_l(t)]\rangle_T, \quad (9)$$

where $\langle \cdots \rangle_T$ stands for the quantum-mechanical and statistical averaging at temperature T.

When substituting $\tilde{\mathcal{H}} = \mathcal{H}$ and $\Gamma_S = 0$ into Eqs. (8) and (9), the function $\mathcal{S}_{\mathrm{res}}$ coincides with the usual incoherent response function $\mathcal{S}_i$ [25,42], which describes incoherent neutron scattering in condensed matter. The approximation $\tilde{\mathcal{H}} \approx \mathcal{H}$ is valid when the mass of the absorbed particle is much smaller than the mass of a target atom or molecule. This is a common and adequate approach when neutron absorption by a much heavier nucleus is considered. However, the mass of a muonic hydrogen atom is comparable to that of a hydrogen-isotope molecule. Thus, the difference (5) between $\tilde{\mathcal{H}}$ and $\mathcal{H}$ cannot be neglected in muonic molecule formation.

Proceeding as in the case of the quasiresonant $dd\mu$-formation process [29] we obtain the following expression for the partial width $\Gamma^{SF}_{\nu_f K_f,\nu_i K_i}$ of back decay of the complex:

$$\Gamma^{SF}_{\nu_f K_f,\nu_i K_i} = 2\pi A_{if} \int \frac{d^3k}{(2\pi)^3} |V_{if}(\varepsilon)|^2 \widetilde{\mathcal{S}}_{\mathrm{res}}(\mathbf{k}, \varepsilon^0_{if} - \varepsilon), \quad (10)$$

where $\widetilde{\mathcal{S}}_{\mathrm{res}}$ denotes the function (8) calculated for the initial state $|\tilde{n}\rangle$, with Γ_S set to zero. The factor A_{if} for the $t\mu$+DC system is

$$A_{if} = \xi \frac{2K_i + 1}{3(2K_f + 1)} q_d,$$

in which $\xi = q_d = 1$ for $C \neq \mathrm{D}$. In the D_2 case, $\xi = \frac{2}{3}$ for even K_i, $\xi = \frac{1}{3}$ for odd K_i, and $q_d = 2$.

In order to compare the calculated formation rates with experiments, the summed formation rate $\lambda^F_{K_i}(\varepsilon)$ is introduced:

$$\lambda^F_{K_i} = \sum_{\nu_f, K_f, S} \lambda^{SF}_{\nu_i K_i \nu_f K_f}, \quad \nu_i = 0. \quad (11)$$

It is convenient to define the effective formation rate $\bar{\lambda}^F_{K_i}(\varepsilon)$ that gives dt fusion. The fusion probability depends on back decay of the created complex. This process competes with deexcitations of the complex that lead finally to dt fusion. If the lifetime of the complex ($\lesssim 1$ ns) is much shorter than its rotational relaxation time, back decay takes place from the initial state K_f. When these times are comparable, it is necessary to include back decay also from lower rotational states

of the complex. In particular, in the limit of very fast rotational relaxation, back decay from the ground rotational state $K_f=0$ is dominant. Such a situation occurs in dense targets, where interactions of the complex with neighboring molecules lead to fast rotational deexcitation. Calculations presented in Refs. [37,38] show that rotational relaxation of the complex, via scattering on neighboring hydrogen-isotope molecules, is fast at liquid hydrogen density. The effective formation rate is then

$$\bar{\lambda}^F_{K_i} = \sum_{K_f,S} \lambda^{SF}_{\nu_i K_i \nu_f K_f} \mathcal{P}^S_{\rm fus}, \quad \nu_i = 0, \tag{12}$$

where $\mathcal{P}^S_{\rm fus}$ is the fusion fraction,

$$\mathcal{P}^S_{\rm fus} = \lambda_f / \Gamma_S,$$

and the total back-decay rate $\lambda^S_{\rm bck}$ in Eq. (2) is given by

$$\lambda^S_{\rm bck} = \sum_{F'} \Gamma_{SF'}, \quad \Gamma_{SF'} = \sum_{\nu'_i} \sum_{K'_i, K_f=0} \Gamma^{SF'}_{\nu_f K_f, \nu'_i K'_i}.$$

It is assumed here that the vibrational level ν_f of the complex is not changed during its lifetime. Estimates of vibrational relaxation for the muonic molecular systems in condensed targets have not been performed yet. However, the available data [28] concerning the $\nu=1\to 0$ relaxation time, for H_2 in solid (8 μs) and liquid (12 μs at 14.2 K) hydrogen, suggest that such times are much greater than the lifetime of a muonic-molecular complex.

B. Formation in a solid in the strong-binding limit

Evaluation of the resonance response function $\mathcal{S}_{\rm res}$ is difficult, in the general case. The first problem is that the operators $\mathbf{R}_l(t)$, $\mathcal{H}$, and $\Delta\mathcal{H}$ in Eq. (9) do not commute [29]. However, when muonic molecule formation takes place at energies significantly smaller than the mean kinetic energy $\mathcal{E}_T$ of molecule DC, the perturbation operator (5) is sufficiently well approximated by its mean value

$$\Delta\mathcal{H} \approx \langle 0|\Delta\mathcal{H}|0\rangle = -\alpha\langle \nabla^2_{R_l}/(2M_{\rm DC})\rangle_T = -\alpha\mathcal{E}_T \equiv \Delta\varepsilon_{if} < 0. \tag{13}$$

Using this approximation in Eq. (9) we obtain

$$\mathcal{Y}_{\rm res}(\mathbf{k},t) \approx \exp(it\Delta\varepsilon_{if})\langle \exp[-i\mathbf{k}\cdot\mathbf{R}_l(0)]\exp[i\mathbf{k}\cdot\mathbf{R}_l(t)]\rangle_T = \exp(it\Delta\varepsilon_{if})\mathcal{Y}_{ll}(\mathbf{k},t).$$

Thus, the function $\mathcal{Y}_{\rm res}$ reduces to the standard incoherent correlation function $\mathcal{Y}_{ll}(\mathbf{k},t)$ [42] multiplied by the factor $\exp(it\Delta\varepsilon_{if})$. This factor describes the variation of the mean target energy due to its mass change. Hence, the formation rate (7) can be written as follows:

$$\lambda^{SF}_{\nu_i K_i, \nu_f K_f} = N_{\rm mol} B_{if} |V_{if}|^2 \int_{-\infty}^{\infty} dt \mathcal{Y}_{ll}(\boldsymbol{\kappa},t) \exp\left[-i\omega t - \frac{1}{2}\Gamma_S |t| \right], \tag{14}$$

where the momentum transfer $\boldsymbol{\kappa}$ and the energy transfer ω to the target are given as

$$\boldsymbol{\kappa} = \mathbf{k}, \quad \omega = \varepsilon - \varepsilon_{if}. \tag{15}$$

The resonance energy ε_{if} in the condensed target is now

$$\varepsilon_{if} = \varepsilon^0_{if} + \Delta\varepsilon_{if}. \tag{16}$$

This energy is shifted by $\Delta\varepsilon_{if}<0$, compared to the free-molecule resonance energy ε^0_{if}.

Similarly, the back-decay width (10) in the strong-binding limit can be expressed in terms of the incoherent response function $\mathcal{S}_i$ introduced by Van Hove [25]. As a result, Eq. (10) takes the simpler form

$$\Gamma^{SF'}_{\nu_f K_f, \nu_i K_i} = 2\pi A_{if} \int \frac{d^3k}{(2\pi)^3} |V_{if}(\varepsilon)|^2 \widetilde{\mathcal{S}}_i(\mathbf{k},\omega'), \tag{17}$$

in which

$$\omega' = \widetilde{\varepsilon}_{if} - \varepsilon, \quad \widetilde{\varepsilon}_{if} = \varepsilon^0_{if} + \Delta\widetilde{\varepsilon}_{if} \tag{18}$$

and

$$\Delta\widetilde{\varepsilon}_{if} \equiv \langle \vec{n}|\Delta\mathcal{H}|\vec{n}\rangle = -(M_{\rm cplx}/M_{\rm DC} - 1)\widetilde{\mathcal{E}}_T < 0, \tag{19}$$

where $\widetilde{\mathcal{E}}_T$ is the mean kinetic energy of the complex in the condensed target. The tilde in $\widetilde{\mathcal{S}}_i$ denotes that the response function is calculated for a target with a bound muonic-molecular complex.

For a perfect gas or a harmonic solid composed of particles with mass $M_{\rm DC}$, the standard correlation function needed for evaluation of Eq. (14) takes a simple Gaussian form [25,42]

$$\mathcal{Y}_{ll}(\boldsymbol{\kappa},t) = \exp\left[-\gamma(t)\frac{\kappa^2}{2M_{\rm DC}} \right]. \tag{20}$$

For a solid with a cubic Bravais structure, the function $\gamma(t)$ is [25]

$$\gamma(t) = \int_0^\infty dw \frac{Z(w)}{w} \left\{ \coth\left(\frac{1}{2}\beta_T w\right)[1-\cos(wt)] - i\sin(wt) \right\}, \tag{21}$$

where $Z(w)$ is the normalized density of vibrational states of the solid and $\beta_T=(k_BT)^{-1}$ (k_B is Boltzmann's constant).

Molecular hydrogen-isotope solids at low pressure, used for studies of muonic atoms and molecules, are quantum molecular crystals. They have the fcc or hcp polycrystalline structure, for which Eq. (21) is a fair approximation [27,28]. As a result, we obtain the so-called phonon expansion for the low-energy $dt\mu$-formation rate in a harmonic crystal:

$$\lambda^{SF}_{\nu_i K_i, \nu_f K_f} = 2N_{\rm mol} B_{if} |V_{if}|^2 \exp(-2W) \times \left[\frac{\Gamma_S}{\omega^2 + \frac{1}{4}\Gamma_S^2} + 2\pi \sum_{n=1}^{\infty} g_{\Gamma n}(\omega) \frac{(2W)^n}{n!} \right], \tag{22}$$

in which

$$g_{\Gamma 1}(w) = \frac{1}{2\pi} \int_{-\infty}^{\infty} dz \frac{\Gamma_S}{z^2 + \frac{1}{4}\Gamma_S^2} g_1(z+w,T),$$

$$g_{\Gamma n}(w) = \int_{-\infty}^{\infty} dw' g_{\Gamma 1}(w - w') g_{n-1}(w') \tag{23}$$

and

$$g_1(w) = \frac{1}{\gamma(\infty)} \frac{Z(w)}{w} [n_B(w) + 1],$$

$$g_n(w) = \int_{-\infty}^{\infty} dw' g_1(w - w') g_{n-1}(w'),$$

$$\int_{-\infty}^{\infty} dw g_n(w) = 1. \tag{24}$$

The exponent $2W$ of the Debye-Waller factor $\exp(-2W)$, familiar in the theory of neutron scattering, is

$$2W(\kappa^2) = \frac{\kappa^2}{2M_{\mathrm{DC}}} \gamma(\infty) = \frac{\kappa^2}{2M_{\mathrm{DC}}} \int_0^{\infty} dw \frac{Z(w)}{w} \coth\left(\frac{1}{2}\beta_T w\right),$$

where $\gamma(\infty)$ stands for the limit of $\gamma(t)$ at $t \to \infty$. The function $n_B(w)$ denotes the Bose factor

$$n_B(w) = [\exp(\beta_T w) - 1]^{-1}.$$

The Breit-Wigner term in the expansion (22) describes recoil-less resonant formation. The sum with higher powers of $2W$ corresponds to quasiresonant muonic molecule formation with simultaneous phonon creation or annihilation. In particular, the term with $n=1$ describes formation connected with the creation or annihilation of one phonon. In the strong-binding limit $2W \ll 1$, only a few of the lowest terms in the expansion (22) are significant. The phonon expansion (22) is more general than an analogous expansion in Ref. [24], which includes the Breit-Wigner factor only in the nonphonon term. This factor should be taken into account also in the phonon terms unless the natural resonance width is much smaller than the maximum crystal frequency. For $2W \gtrsim 1$, the approximation (13) and Eq. (22) are no longer valid.

Let us note that an analogous phonon expansion for $\tilde{\mathcal{S}}_i$ can be applied for estimating the back-decay rate. However, such an approach is valid only if the main contribution to the integral in Eq. (17) comes from small k.

C. Formation in the weak-binding limit

When the incident momentum of a muonic atom is large ($2W \gg 1$), the formation time of a muonic molecule is short compared to the characteristic time scale of dynamic response of the bulk target. Thus, the contribution to the response function (8) from short times is dominant. As a result, it is sufficient to keep only linear terms in t while evaluating the asymptotic form of the correlation function $\mathcal{Y}_{\mathrm{res}}(\mathbf{k},t)$. In calculations, we shall use the following operator relation:

$$\exp(\hat{A})\exp(\hat{B}) = \exp(\hat{A} + \hat{B} + \hat{C}), \tag{25}$$

where

$$\hat{C} = \frac{1}{2}[\hat{A},\hat{B}] + \frac{1}{12}[[\hat{A},\hat{B}],\hat{B}] + \frac{1}{12}[[\hat{B},\hat{A}],\hat{A}] + \frac{1}{24}[[[\hat{B},\hat{A}],\hat{A}],\hat{B}] + \cdots.$$

The operator $\hat{C}=0$ only if $\hat{A}$ and $\hat{B}$ are commuting operators.

The operators $\Delta\mathcal{H}$ and $\mathcal{H}$ do not commute [29] and the operator $\hat{C}$ in the expression

$$\exp\{it(\mathcal{H} + \Delta\mathcal{H})\}\exp(-it\mathcal{H}) = \exp(it\Delta\mathcal{H} + \hat{C})$$

turns out to be a sum containing higher powers of t. Since in this approximation we restrict ourselves to terms linear with respect to t and to the parameter $\alpha \lesssim \frac{1}{2}$, the operator $\hat{C}$ in the above relation can be neglected. Thus, the correlation function takes the form

$$\mathcal{Y}_{\mathrm{res}}(\mathbf{k},t) = \langle \exp\{-i\mathbf{k}\cdot\mathbf{R}_l(0)\}\exp(it\Delta\mathcal{H}) \times \exp\{i\mathbf{k}\cdot\mathbf{R}_l(t)\}\rangle_T. \tag{26}$$

Now we involve the basic approximation

$$\mathbf{R}_l(t) \approx \mathbf{R}(0) + (\mathbf{P}_l/M_{\mathrm{DC}})t, \tag{27}$$

where $\mathbf{P}_l$ denotes the momentum operator of the lth molecule. This approximation is valid for short times. After substitution of Eq. (27) into Eq. (26) and multiple use of Eq. (25) we have

$$\mathcal{Y}_{\mathrm{res}}(\mathbf{k},t) \approx \exp\left(it\frac{k^2}{2M_{\mathrm{cplx}}}\right)\left\langle \exp\left(-it\alpha\frac{P_l^2}{2M_{\mathrm{DC}}}\right)\right\rangle_T \times \left\langle \exp\left(it\frac{\mathbf{k}\cdot\mathbf{P}_l}{M_{\mathrm{cplx}}}\right)\right\rangle_T.$$

Since the argument of the second exponential is small, we can use the following approximation:

$$\left\langle \exp\left(-it\alpha\frac{P_l^2}{2M_{\mathrm{DC}}}\right)\right\rangle_T \approx \exp\left(-it\alpha\left\langle\frac{P_l^2}{2M_{\mathrm{DC}}}\right\rangle_T\right) = \exp(it\Delta\varepsilon_{if}),$$

which involves the resonance-energy shift (13). Substitution of the above equations into Eq. (8), with the definitions (16) and (15) taken into account, leads to

$$\mathcal{S}_{\mathrm{res}}(\boldsymbol{\kappa},\omega) = \frac{1}{2\pi}\int_{-\infty}^{\infty} dt \exp\left[-i\omega t - \frac{1}{2}\Gamma_S|t| + it\frac{\kappa^2}{2M_{\mathrm{cplx}}}\right] \times \left\langle \exp\left(it\frac{\boldsymbol{\kappa}\cdot\mathbf{P}_l}{M_{\mathrm{cplx}}}\right)\right\rangle_T. \tag{28}$$

When the motion of the molecule DC is well described by an isotropic harmonic potential, the Bloch identity

$$\langle \exp\hat{Q}\rangle_T = \exp\left(\tfrac{1}{2}\langle\hat{Q}^2\rangle_T\right) \tag{29}$$

may be applied for the operator $\hat{Q}$ which is a linear combination of the Bose creation and annihilation operators. Since the momentum $\mathbf{P}_l$ can be expressed by such operators (see, e.g., Ref. [42]), we have

$$\left\langle \exp\left(it\frac{\boldsymbol{\kappa}\cdot\mathbf{P}_l}{M_{\mathrm{cplx}}}\right)\right\rangle_T = \exp\left(-\frac{1}{4}\Delta_{\mathrm{res}}^2\right),$$

$$\Delta_{\mathrm{res}}^2 = \frac{2}{M_{\mathrm{cplx}}^2}\langle(\boldsymbol{\kappa}\cdot\mathbf{P}_l)^2\rangle_T. \tag{30}$$

In the case of cubic symmetry,

$$\langle(\boldsymbol{\kappa}\cdot\mathbf{P}_l)^2\rangle_T = \tfrac{1}{3}\kappa^2\langle P_l^2\rangle_T,$$

and this is a fair approximation even for other lattices. Thus

$$\Delta_{\mathrm{res}}^2 = \frac{2}{3M_{\mathrm{cplx}}^2}\kappa^2\langle P_l^2\rangle_T = \frac{8}{3}\frac{M_{\mathrm{DC}}}{M_{\mathrm{cplx}}}\left\langle\frac{P_l^2}{2M_{\mathrm{DC}}}\right\rangle_T\frac{\kappa^2}{2M_{\mathrm{cplx}}},$$

which finally gives the following Doppler width:

$$\Delta_{\mathrm{res}} = 2\sqrt{\frac{2}{3}\frac{M_{\mathrm{DC}}}{M_{\mathrm{cplx}}}\mathcal{E}_T\omega_R}, \tag{31}$$

with the recoil energy

$$\omega_R = \kappa^2/(2M_{\mathrm{cplx}}). \tag{32}$$

In the case of a solid hydrogen target, the mean kinetic energy of a bound molecule equals

$$\mathcal{E}_T = \tfrac{3}{2}\int_0^\infty dwZ(\omega)w\left[n_B(\omega)+\tfrac{1}{2}\right]. \tag{33}$$

This energy is much higher than $\mathcal{E}_T=\frac{3}{2}k_BT$ for a corresponding Maxwellian gas, unless the temperature is sufficiently high. In particular, for a low-pressure solid or liquid deuterium, $\mathcal{E}_T\approx 5$ meV [43] due to large zero-point motion of the D_2 molecules. The effective target temperature T_{eff} corresponding to $\mathcal{E}_T$ is then defined as

$$T_{\mathrm{eff}} \equiv \tfrac{2}{3}k_B^{-1}\mathcal{E}_T. \tag{34}$$

For the solid-D_2 case considered here, $T_{\mathrm{eff}}\approx 40$ K.

Substitution of Eqs. (30) and (32) into Eq. (28) leads to

$$\mathcal{S}_{\mathrm{res}}(\boldsymbol{\kappa},\omega) = \frac{1}{2\pi}\int_{-\infty}^{\infty}dt\,\exp\left[-i(\omega-\omega_R)t-\frac{1}{2}\Gamma_S|t|-\frac{1}{4}\Delta_{\mathrm{res}}^2t^2\right]. \tag{35}$$

Then, applying the convolution theorem for the Fourier transform of a product, we obtain the asymptotic form of the resonance response function:

$$\mathcal{S}_{\mathrm{res}}(\boldsymbol{\kappa},\omega) = \frac{1}{2\pi^{3/2}}\frac{\Gamma_S}{\Delta_{\mathrm{res}}}\int_{-\infty}^{\infty}\frac{dz}{z^2+\frac{1}{4}\Gamma_S^2}\times\exp\left[-\left(\frac{z+\omega-\omega_R}{\Delta_{\mathrm{res}}}\right)^2\right]. \tag{36}$$

By virtue of Eq. (36), the formation rate (7) takes the form

$$\lambda^{SF}_{\nu_iK_i,\nu_fK_f} = N_{\mathrm{mol}}B_{if}|V_{if}|^2\frac{\Gamma_S}{\Delta_{\mathrm{res}}\sqrt{\pi}}\times\int_{-\infty}^{\infty}\frac{dz}{z^2+\frac{1}{4}\Gamma_S^2}\exp\left[-\left(\frac{z+\omega-\omega_R}{\Delta_{\mathrm{res}}}\right)^2\right], \tag{37}$$

in the weak-binding limit. This equation is similar (apart from the muonic-molecule factor $N_{\mathrm{mol}}B_{if}|V_{if}|^2$) to the expression for resonant absorption of neutrons in a gas target, obtained by Bethe and Placzek [44]. However, the resonance width (31) and recoil energy (32) take into account the change of the target particle mass in the absorption process, which is neglected in their work.

In the limit $\Gamma_S\to 0$, Eqs. (36) and (37) tend to the following expressions:

$$\mathcal{S}_{\mathrm{res}}(\boldsymbol{\kappa},\omega) = \frac{1}{\Delta_{\mathrm{res}}\sqrt{\pi}}\exp\left[-\left(\frac{\omega-\omega_R}{\Delta_{\mathrm{res}}}\right)^2\right] \tag{38}$$

and

$$\lambda^{SF}_{\nu_iK_i,\nu_fK_f} = 2\sqrt{\pi}N_{\mathrm{mol}}B_{if}|V_{if}|^2\frac{1}{\Delta_{\mathrm{res}}}\exp\left[-\left(\frac{\omega-\omega_R}{\Delta_{\mathrm{res}}}\right)^2\right], \tag{39}$$

respectively. The function (38) has the Gaussian form, identical with that used for the description of incoherent scattering at large energies. However, the Doppler width (31) and the recoil energy (32) in $\mathcal{S}_{\mathrm{res}}$ are different from the corresponding variables

$$\Delta_R = 2\sqrt{\tfrac{2}{3}\mathcal{E}_T\omega_R} \tag{40}$$

and

$$\omega_R = \kappa^2/(2M_{\mathrm{DC}}), \tag{41}$$

which determine the asymptotic form of the standard incoherent response function $\mathcal{S}_i$ [42]. The function (38) tends to $\mathcal{S}_i$ if the approximation $M_{\mathrm{cplx}}\approx M_{\mathrm{DC}}$ is valid. In the case of muonic molecule formation, this is only a rough approximation.

Equation (38) can be used for the evaluation of the backdecay rate if large final momenta give the main contribution to the integral (10). After integration over direction of $\mathbf{k}$ in Eq. (10), with the asymptotic function (38) inserted, one obtains

$$\Gamma^{SF'}_{\nu_fK_f,\nu_iK_i} = \frac{A_{if}}{\pi^{3/2}\tilde{\Delta}_{\mathrm{res}}}\int_0^\infty dkk^2|V_{if}(\varepsilon)|^2\exp\left[-\left(\frac{\omega'-\omega_R'}{\tilde{\Delta}_{\mathrm{res}}}\right)^2\right], \tag{42}$$

where ω' is defined by Eq. (18). The parameters $\tilde{\Delta}_{\mathrm{res}}$ and ω_R' are calculated from Eqs. (31) and (32), using the substitutions $M_{\mathrm{DC}}\leftrightarrow M_{\mathrm{cplx}}$ and $\mathcal{E}_T\to\tilde{\mathcal{E}}_T$.

Let us note that Eqs. (36) and (38) are general since they are derived in the impulse approximation (27) without using specific properties of a given target, apart from the single parameter $\mathcal{E}_T$. Therefore, they are valid for liquid and dense

gaseous hydrogen isotopes. They can also be used for describing resonant absorption processes other than muonic molecule formation, when the mass change cannot be neglected. In such a case, Γ_S should be replaced by the appropriate resonance width.

D. Formation in a solid at intermediate energies

The formation rate calculated according to the asymptotic form (37) is very inaccurate unless $2W \gg 1$. In particular, this concerns the contribution to the rate from recoil-less formation, which is important at low energies. Therefore, at $2W \sim 1$, it is reasonable to represent the formation rate as a sum of the exact recoil-less Breit-Wigner term from Eq. (22) and the phonon contributions that we obtain below in the impulse approximation. Using Eqs. (25) and (29), it can be shown that the relation

$$\mathcal{Y}_{ll}^{\mathrm{res}}(\mathbf{k},t) \approx \mathcal{Y}_{ll}(\mathbf{k},t)\exp(it\Delta\varepsilon_{if})\exp\left\{\alpha\left[it - \frac{2}{3}(\alpha + 2)\mathcal{E}_T t^2\right]\frac{k^2}{2M_{\mathrm{DC}}}\right\} \tag{43}$$

is valid in this approach. Inserting Eqs. (20) and (43) into Eq. (8) we have

$$\mathcal{S}_{\mathrm{res}}(\boldsymbol{\kappa},\omega) = \frac{1}{2\pi}\int_{-\infty}^{\infty} dt\, \exp\left\{-it\omega - \frac{1}{2}\Gamma_S|t| + \left[-\gamma(t) + i\alpha t - \frac{2}{3}\alpha(\alpha+2)\mathcal{E}_T t^2\right]\frac{\kappa^2}{2M_{\mathrm{DC}}}\right\}. \tag{44}$$

Substituting the approximation $\gamma(t) \approx -it + \frac{2}{3}\mathcal{E}_T t^2$ for short times into Eq. (44) and integrating over t yields the asymptotic form (36) of the response function. However, we now expand Eq. (44) in powers of κ^2:

$$\mathcal{S}_{\mathrm{res}}(\boldsymbol{\kappa},\omega) = \frac{1}{2\pi}\exp(-2W)\sum_{n=0}^{\infty}\frac{(2W)^n}{n!} \times \int_{-\infty}^{\infty} dt\, \exp\left(-i\omega t - \frac{1}{2}\Gamma_S|t|\right)[\mathcal{F}(t)]^n,$$

$$\mathcal{F}(t) = 1 + i\frac{1+\alpha}{\gamma(\infty)}t - \frac{2}{3}\frac{(1+\alpha)^2}{\gamma(\infty)}\mathcal{E}_T t^2. \tag{45}$$

The function g_n is defined by Eq. (24). The integral over t is estimated using the exponential approximation to the function $\mathcal{F}$:

$$\mathcal{F}(t) \approx \exp(x), \quad x \approx \frac{it}{\gamma_\alpha} - \frac{1}{2}\Delta_\alpha^2 t^2, \tag{46}$$

where x contains only leading terms in t and

$$\gamma_\alpha \equiv \frac{M_{\mathrm{cplx}}}{M_{\mathrm{DC}}}\gamma(\infty), \quad \Delta_\alpha^2 \equiv \frac{4}{3}\frac{M_{\mathrm{DC}}}{M_{\mathrm{cplx}}}\frac{\mathcal{E}_T}{\gamma_\alpha} - \frac{1}{\gamma_\alpha^2}.$$

Then, integration in Eq. (45) by using the convolution theorem leads to

$$\mathcal{S}_{\mathrm{res}}(\boldsymbol{\kappa},\omega) = \exp(-2W)\left[\frac{1}{2\pi}\frac{\Gamma_S}{\omega^2 + \frac{1}{4}\Gamma_S^2} + \sum_{n=1}^{\infty}\mathfrak{g}_n(\omega)\frac{(2W)^n}{n!}\right], \tag{47}$$

where

$$\mathfrak{g}_1(\omega) = \frac{1}{2\pi}\int_{-\infty}^{\infty} dz \frac{\Gamma_S}{z^2 + \frac{1}{4}\Gamma_S^2}\frac{Z(z+\omega_\alpha)}{z+\omega_\alpha} \times [n_B(z+\omega_\alpha)+1], \quad \omega_\alpha = \frac{\omega}{1+\alpha},$$

and, for $n \geq 2$,

$$\mathfrak{g}_n(\omega) = \frac{1}{(2\pi)^{3/2}}\frac{\Gamma_S}{n^{1/2}\Delta_\alpha}\int_{-\infty}^{\infty} dz \frac{1}{z^2 + \frac{1}{4}\Gamma_S^2} \times \exp\left[\frac{(z+\omega-n/\gamma_\alpha)^2}{2n\Delta_\alpha^2}\right].$$

The first term of Eq. (45) has been replaced in Eq. (47) by the exact Breit-Wigner term. Also, the one-phonon ($n=1$) contribution to $\mathcal{S}_{\mathrm{res}}$ is replaced here by a more accurate term depending on $\mathfrak{g}_1$. The function $\mathfrak{g}_1$ is calculated by substituting the exact function $\gamma(t)$ for a harmonic solid into Eq. (44). Every multiphonon term in Eq. (47) is represented by the convolution of the Breit-Wigner profile with a Gaussian obtained using Eq. (46). It thus follows that

$$\lambda^{SF}_{\nu_i K_i, \nu_f K_f} = N_{\mathrm{mol}} B_{if}|V_{if}|^2 \exp(-2W) \times \left[\frac{\Gamma_S}{\omega^2 + \frac{1}{4}\Gamma_S^2} + 2\pi\sum_{n=1}^{\infty}\mathfrak{g}_n(\omega)\frac{(2W)^n}{n!}\right]. \tag{48}$$

The form of this expansion is similar to that of Eq. (22), derived in the strong-binding limit. However, the functions $\mathfrak{g}_n$ are obtained in the impulse approximation and they are different from the corresponding functions $g_{\Gamma n}$ given by Eq. (23). For the one-phonon term, we have $\mathfrak{g}_1(\omega) = g_{\Gamma 1}(\omega_\alpha)$, which is the direct result of using the exact $\gamma(t)$ in derivation of $\mathfrak{g}_1$. Thus, Eqs. (48) and (22) give the same rate at smallest energy transfers. At large ε, when many multiphonon terms are important, the target response no longer displays a rich structure. The rate (48) therefore tends to the simpler form (37), which is characterized by the recoil energy (32) with the correct mass M_{cplx}.

In the limit $\Gamma_S \to 0$, the rate (48) takes the form

$$\lambda^{SF}_{\nu_i K_i, \nu_f K_f} = 2\pi N B_{if}|V_{if}|^2 \exp(-2W) \times \left[\delta(\omega) + \sum_{n=1}^{\infty}\mathfrak{g}_n(\omega,T)\frac{(2W)^n}{n!}\right], \tag{49}$$

with the expansion coefficients

$$\mathfrak{g}_1(\omega) = \frac{Z(\omega_\alpha)}{\omega_\alpha}[n_B(\omega_\alpha) + 1],$$

$$\mathfrak{g}_n(\omega) = \frac{1}{(2\pi n)^{1/2}\Delta_\alpha} \exp\left[\frac{(\omega - n/\gamma_\alpha)^2}{2n\Delta_\alpha^2}\right], \quad n \geqslant 2.$$

The contribution from intermediate final momenta to the back-decay rate (10) can be calculated analogously.

IV. RESULTS OF CALCULATIONS FOR $dt\mu$ FORMATION IN HYDROGEN-ISOTOPE CRYSTALS

In this section, the rates of resonant $dt\mu$ formation in solid HD, D_2, and DT are calculated. It is assumed that these targets are kept at zero or low pressure ($\ll$10 kbar), which corresponds to the TRIUMF or RIKEN-RAL experimental conditions. Measurements of the formation rates at TRIUMF have been performed using energetic ($\sim$1 eV) beams of $t\mu$ atoms. Therefore, the rates are evaluated here in a wide energy interval $\varepsilon \lesssim 1$ eV. This involves resonant $dt\mu$ formation with simultaneous excitations of the few lowest vibrational levels of the muonic-molecular complex. The values of the rates are given for a normalized target density of 4.25×10^{22} atoms/cm^3 (liquid-hydrogen density).

Since the exact form of the vibrational-state distribution $Z(w)$ for the experimental polycrystalline targets is not known, the Debye model of an isotropic solid has been used in the calculations presented below. The values of the Debye temperature Θ_D are taken from the available literature [27,28].

The resonance energies and energy-dependent transition-matrix elements for isolated target molecules HD, D_2, and DT, calculated according to the method presented in Ref. [45], are the starting point for the evaluation of the formation rates in solid hydrogen isotopes. The transition-matrix elements are available for the rotational transitions $K_i=0, 1 \to K_f=0,\ldots,9$.

Resonant $dt\mu$ formation in a bound D_2 molecule is the most complicated case. The lowest resonances, corresponding to the vibrational transition $\nu_i=0 \to \nu_f=2$ and different rotational states K_i and K_f, are located in the vicinity of $\varepsilon=0$ with a radius of a few dozen meV. The resonance energies in this region for a free D_2 molecule and for a D_2 bound in a 3-K solid deuterium are shown in Table I. In particular, there are several subthreshold resonances that give significant contributions to the low-energy rates because of wide resonance profiles. The resonance-energy shift (13) for a 3-K deuterium target is $\Delta\varepsilon_{if}=-2.29$ meV. Resonances in the upper spin state $F=1$ have much smaller energies than those for $F=0$ with the same rotational quantum numbers. In particular, the largest values of ε_{if} for $F=1$, shown in Table I, are due to the excitations $K_i=0, 1 \to K_f=4$. The only matrix elements which do not tend to zero at $\varepsilon \to 0$ correspond to the dipole transitions $K_i=0 \to K_f=1$ and $K_i=1 \to K_f=0,2$. For $F=1$, all these transitions are associated with $\varepsilon_{if} < -50$ meV and thus give very small contributions to the $dt\mu$-formation rate. As a result, the low-energy rate is determined mainly by $t\mu$ scattering in the $F=0$ state. However, even for $F=0$, dipole transitions are connected with negative resonance energies, though much closer to $\varepsilon=0$ than in the $F=1$ case. The lowest positive resonances appear in the transitions $K_i=0 \to K_f=3,4$ and $K_i=1 \to K_f=3,4$. They are characterized by strongly varying transition-matrix elements [45], which are illustrated in Figs. 3 and 4 (the matrix elements shown below are given in atomic units $e=\hbar=m_e=1$). Let us note that this situation is very different from the $dd\mu$ case, where low-energy formation is determined by dipole transitions, with the matrix elements slowly varying below a few dozen meV [29,45]. Another difference between the $dd\mu$ and $dt\mu$ cases is due to large separations of the low-energy $dt\mu$ resonances corresponding to $K_i=0$ and $K_i=1$. In the $dd\mu$ case, the energies of such resonances are much closer. There-

TABLE I. The resonance energies for $dt\mu$ formation in $t\mu$ scattering from single a D_2 molecule (ε_{if}^0) and from a 3-K solid-D_2 target (ε_{if}), for the vibrational transition $\nu_i=0 \to \nu_f=2$. These energies are given in the corresponding center-of-mass systems.

ε_{if}^0 (meV)	ε_{if} (meV)	F	K_i	K_f	S
−25.66	−27.95	1	1	4	1
−21.25	−23.54	1	0	4	0
−18.66	−20.95	1	1	4	2
−18.25	−20.54	1	0	4	1
−11.25	−13.54	1	0	4	2
−24.15	−26.44	0	1	0	1
−19.28	−21.57	0	1	1	1
−16.74	−19.02	0	0	0	1
−11.86	−14.15	0	0	1	1
−9.547	−11.84	0	1	2	1
−2.133	−4.423	0	0	2	1
5.007	2.718	0	1	3	1
12.42	10.13	0	0	3	1
24.34	22.05	0	1	4	1
31.75	29.46	0	0	4	1

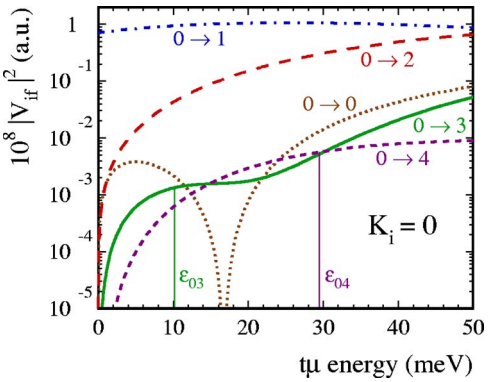

FIG. 3. (Color online) Transition-matrix elements $|V_{if}(\varepsilon)|^2$ versus $t\mu$ energy for the transitions $K_i=0 \to K_f=0,1,2,3,4$ and $\nu_i=0 \to \nu_f=2$. The vertical lines denote energies ε_{if} of the lowest resonances. Labels "$i \to f$" stand for the rotational transitions $K_i \to K_f$.

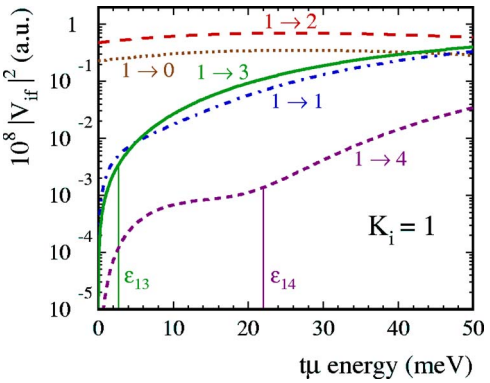

FIG. 4. (Color online) Transition-matrix elements $|V_{if}(\varepsilon)|^2$ versus $t\mu$ energy for the transitions $K_i=1\rightarrow K_f=0,1,2,3,4$ and $\nu_i=0\rightarrow\nu_f=2$. Notation is the same as in Fig. 3.

fore, for $dt\mu$ one can expect more pronounced differences between resonant formation in solid ortho-D_2 and para-D_2 than those found for the $dd\mu$ case [46]. Most pure-deuterium experiments in μCF have been carried out in targets with the statistical mixture of ortho and parastates (called "normal" deuterium nD_2, according to the nomenclature used in Ref. [28]).

Figure 5 shows $|V_{if}(\varepsilon)|^2$ for the transition $\nu_i=0\rightarrow\nu_f=2$ and $K_i=1\rightarrow K_f=3$, together with the response function (47) for the resonance $F=0\rightarrow S=1$ located at $\varepsilon_{if}=2.7$ meV. The phonon terms in $\mathcal{S}_{\rm res}$ are calculated assuming $\Gamma_S=0$, since in this example we want to neglect their convolution with the Breit-Wigner profile. There is a strong contrast between resonant formation of the molecules $dt\mu$ and $dd\mu$ [29] in solid deuterium. In the $dt\mu$ case, the wide Breit-Wigner peak is not so much pronounced as the narrow recoil-less $dd\mu$ resonances. The matrix element $|V_{if}(\varepsilon)|^2$ increases by a few orders of magnitude within the width of 100 meV of the multiphonon distribution. Thus, the phonon contribution to the $dt\mu$-formation rate is comparable with the nonphonon one, already above a few meV. This means that the detailed form of the density $Z(w)$ of vibrational lattice states is necessary

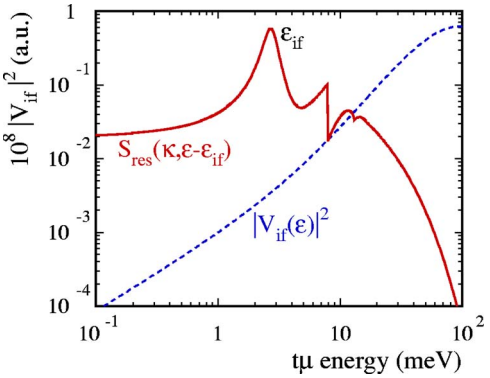

FIG. 5. (Color online) Transition-matrix element $|V_{if}(\varepsilon)|^2$ for resonant $dt\mu$ formation (transition $\nu_i=0\rightarrow\nu_f=2$, $K_i=1\rightarrow K_f=3$, dashed line) and the response function $\mathcal{S}_{\rm res}(\boldsymbol{\kappa},\varepsilon-\varepsilon_{if})$ (in arbitrary units, solid line) for the resonance $F=0\rightarrow S=1$ in a 3-K para-D_2. The peak of the Breit-Wigner term from Eq. (47) is centered at the resonance energy $\varepsilon_{if}=2.7$ meV.

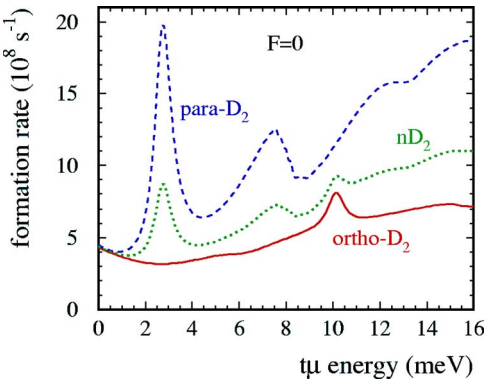

FIG. 6. (Color online) Low-energy $dt\mu$-formation rate for $F=0$ in a 3-K solid nD_2 ("normal" deuterium [28]), ortho-D_2, and para-D_2, calculated using Eq. (48).

for the accurate calculation of the low-energy $dt\mu$-formation rate in a solid D_2. The shape of the vibrational spectrum in the energy-dependent rate is strongly distorted, which can be seen in Fig. 6 evaluated using Eq. (48). Nevertheless, the one-phonon and two-phonon terms are clearly distinguished in the curve corresponding to para-D_2. In ortho-D_2, a resonance with the lowest $\varepsilon_{if}>0$ is located at 10 meV. Therefore, the Breit-Wigner peak is strongly suppressed by the Debye-Waller factor and the rate is quite flat. At $\varepsilon\rightarrow 0$, the rates are determined by the wings of the Breit-Wigner peaks, because the phonon contribution to the rates vanishes when κ approaches zero. For $F=1$, the main resonances are far from the considered low-energy interval (see Table I). The rates shown in Fig. 7 are thus determined by the Breit-Wigner wings of the deep subthreshold resonances with a small contribution from the weak resonance ($K_f=5$) located at $\varepsilon_{if}>0$. As a result, the formation rates for $F=1$ are lower by two orders of magnitude than those for $F=0$.

Resonances in $t\mu$ scattering from D_2, corresponding to the vibrational excitations $\nu_f\geqslant 3$ of the $[(dt\mu)dee]$ complex, are located at higher energies $\varepsilon\gtrsim 0.2$ eV. Therefore, they are well described by the asymptotic form (37), which is independent of $Z(w)$. Therefore, the formation rate is determined accurately using only the mean kinetic energy $\mathcal{E}_T$ of the D_2 molecule. The formation rate in 3-K solid nD_2 is plotted in Fig. 8, for several ν_f. For comparison, Fig. 9 shows the

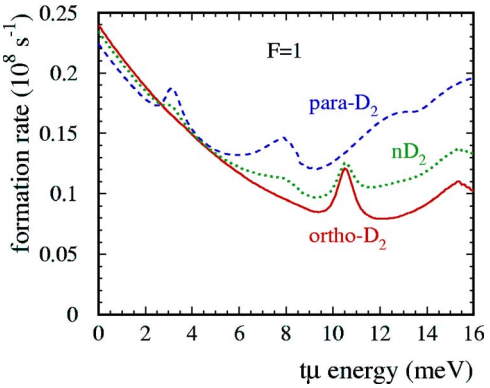

FIG. 7. (Color online) Low-energy $dt\mu$-formation rate for $F=1$ in the same targets as in Fig. 6.

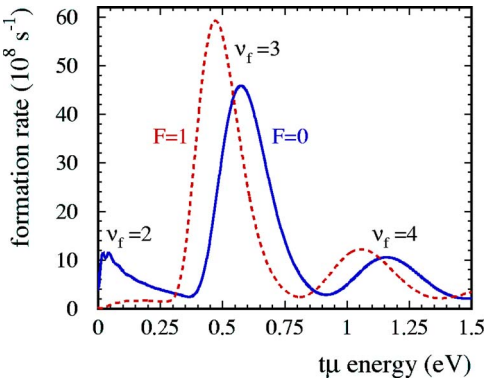

FIG. 8. (Color online) Resonant $dt\mu$-formation rate in a 3-K solid nD_2 for $F=0$ and $F=1$. The label ν_f denotes the vibrational state of the created $[(dt\mu)dee]$ complex.

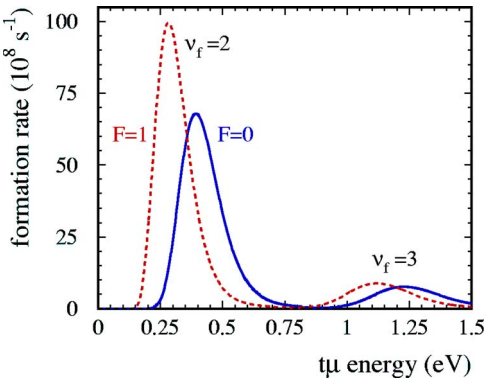

FIG. 10. (Color online) Resonant $dt\mu$-formation rate in a 3-K solid HD.

$dt\mu$-formation rate for a 3-K gaseous nD_2. The energy-dependent rate for a perfect deuterium gas has been calculated assuming a 3-K Maxwellian distribution of the D_2 kinetic energy. This rate includes only formation due to two-body $t\mu+D_2$ collisions. The resonant-formation rates presented in Figs. 8 and 9 display a striking difference between the gas and the solid case. At $\varepsilon\to 0$, the theory developed for two-body collisions in a perfect gas gives a negligible resonant formation rate. This result disagrees with the average formation rates determined by measurements performed in liquid and cold dense-gas targets [3] and in solid [18] targets. The rate for the solid shows a strong contribution from the subthreshold resonances, which leads to a large rate in the limit $\varepsilon\to 0$. Solid-state effects are also significant at higher energies. The resonance peaks in a solid are much broader than those in the gas because of the large effective target temperature [43]. The widths of the peaks increase with rising recoil energy. However, the centers of higher-energy peaks in both targets have similar locations since, in the impulse-approximation limit, the recoil energy (32) for the muonic-molecular complex bound in a solid equals that for the isolated complex. The small difference $\Delta\varepsilon_{if}$ of the resonance energy between the solid and the gas is negligible for $\varepsilon_{if}\gg 1$ meV.

Calculation of the $dt\mu$-formation rate for solid HD or DT is simpler than for D_2 since in the HD or DT case there are no significant resonances in the close vicinity of $\varepsilon=0$. This is caused by different values of the rotational and vibrational quanta for these molecules. The HD molecule is the lightest one and the resonances connected with $\nu_f=2$ are situated in HD above 0.1 eV [14,45]. As a result, the contributions from various multiphonon processes to the formation rate plotted in Fig. 10 cannot be distinguished. The resonance peak for $\nu_f=2$ in HD is the strongest $dt\mu$ resonance found for the three molecules considered here.

In Fig. 11, the $dt\mu$-formation rate is shown for a 3-K solid DT target. The lowest peaks, which already take the asymptotic form (37), correspond here to $\nu_f=3$. The rotational and vibrational quanta are smallest for DT, so that the main (lowest K_f) resonances connected with $\nu_f=2$ are located deeply below $\varepsilon=0$. Thus, the contribution to the formation rate from the subthreshold resonances is very small and not apparent in this figure. At 3 K, the effective target temperature T_{eff}, determined by Eqs. (34) and (33), equals about 41 K for HD and 50 K for DT. The resonance shift $\Delta\varepsilon_{if}$ obtained from Eq. (13) equals −2.71 meV in the case of HD and −1.97 meV for DT.

The $dt\mu$ resonances in solid HD and D_2 were directly observed at TRIUMF [19–22] using the energetic $t\mu$-atom beam and time-of-flight techniques. However, Monte Carlo simulations (see, e.g., Ref. [47]) were employed for interpreting the experimental data. Such a procedure was indispensable since the time-of-flight spectra cannot be uniquely

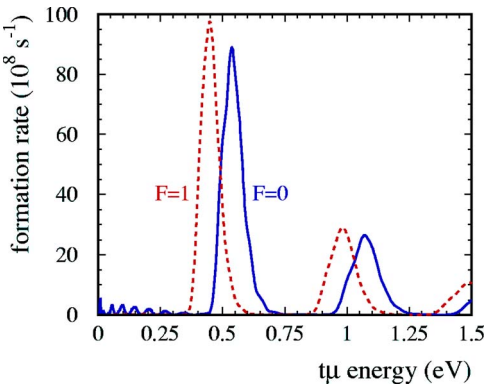

FIG. 9. (Color online) Resonant $dt\mu$-formation rate in 3-K gaseous nD_2 calculated in the laboratory frame.

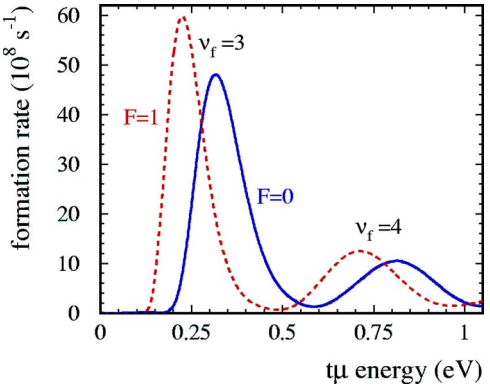

FIG. 11. (Color online) Resonant $dt\mu$-formation rate in a 3-K solid HT.

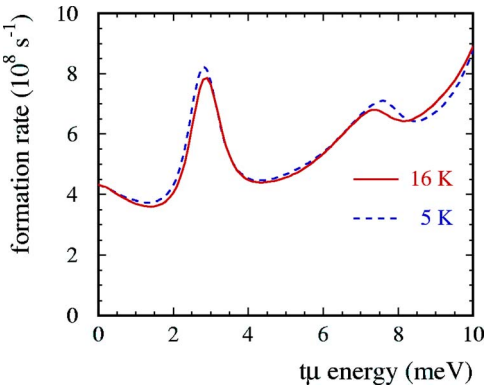

FIG. 12. (Color online) Rate of resonant $dt\mu$ formation in $t\mu(F=0)$ scattering from a D_2 molecule bound in 5-K and 16-K solid D/T(C_t=0.4) targets.

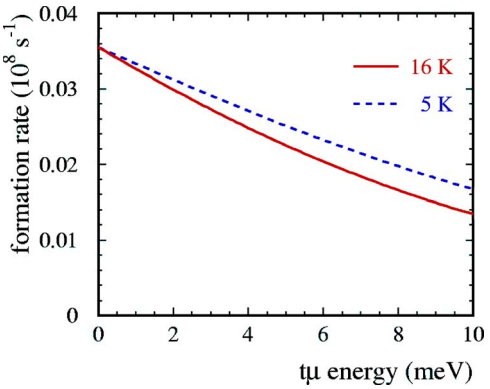

FIG. 13. (Color online) Rate of resonant $dt\mu$ formation in $t\mu(F=0)$ scattering from a DT molecule bound in 5-K and 16-K solid D/T(C_t=0.4) targets.

inverted because of the geometry used and the energy loss of $t\mu$ atoms in the reaction layer prior to resonant formation of the muonic-molecular complex. In those simulations, the calculated $dt\mu$-formation rates for 3-K gas targets (such as that shown in Fig. 9) were applied because the theoretical formation rates for a low-pressure solid were not available. A detailed analysis of the data was performed by Fujiwara [19]. He found more dt-fusion events at lowest and highest $t\mu$ energies than had been predicted using the perfect gas model. Much broader resonance peaks, which we present in Fig. 8, can certainly improve fits to the TRIUMF data. Also, the analysis of the fusion-product yield [19] proved that the low-energy $dt\mu$-formation rate in solid deuterium was much higher than that predicted by the two-collision gas model. In particular, this concerns formation for the state $F=1$. The theoretical rates presented in Fig. 7 support this finding.

The two-peak structure of the calculated time-of-flight spectra for $dt\mu$ resonances in HD, obtained assuming a 3-K gas model, was not confirmed by the solid-HD data [21]. However, one may expect much better agreement with the TRIUMF data when the rate shown in Fig. 10 is used instead of the very pronounced peaks evaluated for 3-K HD gas. A possibility of wider resonance peaks with a fixed Doppler width of 50 meV was already considered in Ref. [21], which did not give good fits to the data. Such a result is now explainable since, according to Eq. (31), the Doppler width of a resonance in a condensed target increases with the rising recoil energy ω_R. Simultaneously, the resonance height (37) decreases for higher ω_R so that the resonance strength is preserved.

Figures 12 and 13 show the resonant-formation rates for molecules D_2 and DT bound in a solid D/T target. An equilibrated mixture of molecules D_2, DT, and T_2 is assumed for a tritium isotopic concentration C_t=0.4. Target temperatures 5–16 K were applied in the RIKEN-RAL experiment, in which an unexpected temperature dependence of the $dt\mu$-formation rate in solid D-T mixtures [18] was found. The corresponding target density is almost constant. A similar hydrogen-isotope mixture, kept at 15 K, was also used in the PSI experiment [4]. In both experiments, time spectra of neutrons from dt fusion were measured. The data were interpreted using standard steady-state kinetics, assuming that the $t\mu$ atoms were thermalized. Formation from the state $F=1$ is negligible for an appreciable tritium concentration as the spin-flip transition $F=1\rightarrow 0$ in low-energy $t\mu+t$ collisions is very fast [48]. The theoretical energy-dependent $dt\mu$-formation rates display a weak temperature dependence. One can expect such a behavior since, for any temperature of a low-pressure hydrogen-isotope solid, the limit $T/\Theta_D \ll 1$ is achieved ($\Theta_D \approx 100$ K) and changes of Θ_D are very small [27,28]. As a result, the response function (47) and thus the formation rate (48) are always close to their limits for $T/\Theta_D \rightarrow 0$. Therefore, changes of the average formation rate $\tilde{\lambda}_{dt\mu}$, determined using steady-state conditions, can only be ascribed to different $t\mu$-energy distributions corresponding to various target temperatures. An accurate comparison of the theory with data requires Monte Carlo simulations of the μCF cycle in a given solid D-T mixture, which can be performed in the future after completing the full set of differential cross section for muonic atom scattering in mixed D-T crystals. The $t\mu$-energy distribution in steady-state conditions is a crucial information. The shape of such a distribution is non-Maxwellian and the mean $t\mu$ energy is greater than $\frac{3}{2}k_BT$, due to solid-state effects and to a possible admixture of epithermal $t\mu$'s from the reaction $d\mu+t\rightarrow t\mu+d$ and from back decay of the muonic-molecular complex. The latter effect was studied in Refs. [35,49] with the use of Monte Carlo simulations in the case of gaseous and liquid targets. In a high-density target with medium or high C_t, this effect is small, which is confirmed by the PSI fits [4].

Averaging the energy-dependent rate from Fig. 12 over the kinetic-energy distribution of $t\mu(F=0)$ leads to the mean resonant rate $\tilde{\lambda}^0_{dt\mu}$ shown in Fig. 14. The energy distribution of $t\mu$ atoms, being in thermal equilibrium with phonons, is assumed to be proportional to $Z(\varepsilon)n_B(\varepsilon,T)$. The average $t\mu$ energy obtained using this function ranges from 1.2 meV for T=5 K to 3.4 meV for T=16 K. It is evident that the rise of the formation rate above about 3 K is mainly due to $t\mu$ atoms entering into the region of the recoil-less resonant peak in para-D_2, centered at 2.7 meV. Phonon processes in both ortho-D_2 and para-D_2 lead to a smaller rise in the rate. The calculated formation rate is close to the PSI result for T =13 K [4]. Coincidence of the theoretical curve with the data is obtained, as in the case of the TRIUMF measurements

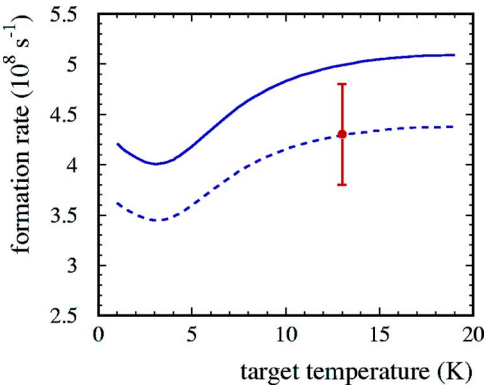

FIG. 14. (Color online) Mean rate of resonant $dt\mu$ formation in $t\mu(F=0)$ scattering from nD_2 molecules bound in solid D-T ($C_t=0.4$) as a function of the target temperature. The dashed line represents the same rate scaled by the factor $S_\lambda=0.86$. Also shown is the result of the PSI measurement [4] for a similar target ($T=13$ K, $\varphi=1.45$).

[20], upon scaling by a factor $S_\lambda<1$, which can be ascribed to the inaccuracy of the calculated transition-matrix elements. Here, we find $S_\lambda=0.86$, which is consistent with the result of Ref. [20].

In the RIKEN-RAL experiment [18], about a 20% decrease of the μCF effectiveness has been found for the target-temperature change from 16 to 5 K, independently of the tritium concentration. In order to explain this effect, several hypotheses have been considered. The hypothesis of a significant change of the mean resonant $dt\mu$ formation rate for $F=0$ has led to the best fits to the data. Kawamura *et al.* assume that the two components of $\tilde{\lambda}^0_{dt\mu}$—namely, the rate $\tilde{\lambda}^{0,D_2}_{dt\mu}$ of resonant formation for the D_2 molecule and the analogous rate $\tilde{\lambda}^{0,DT}_{dt\mu}$ for the DT molecule—are comparable. At 16 K, they use $\tilde{\lambda}^{0,D_2}_{dt\mu}=3.5\times10^8$ s^{-1} and $\tilde{\lambda}^{0,DT}_{dt\mu}=1.6\times10^8$ s^{-1} [18]. All the temperature dependence of $\tilde{\lambda}^0_{dt\mu}\equiv C_d\tilde{\lambda}^{0,D_2}_{dt\mu}+C_t\tilde{\lambda}^{0,DT}_{dt\mu}$ (C_d is the deuterium isotopic concentration) is ascribed only to $\tilde{\lambda}^{0,D_2}_{dt\mu}$. With the other rates in the steady-state kinetics being fixed, about a 30% decrease of $\tilde{\lambda}^{0,D_2}_{dt\mu}$ between 16 K and 5 K has been obtained. Thus, for $C_t=0.4$, the respective change of $\tilde{\lambda}^0_{dt\mu}$ equals about 25%. This finding agrees quite well with analogous 20% decrease of the theoretical rate plotted in Fig. 14. However, theory predicts that the low-energy rate $\tilde{\lambda}^{0,DT}_{dt\mu}$ should be smaller by a few orders of magnitude than the corresponding rate $\tilde{\lambda}^{0,D_2}_{dt\mu}$, since the strong resonances in $t\mu$+DT scattering are far from the region $\varepsilon\approx0$. Averaging the rate presented in Fig. 13 over the $t\mu$-energy distribution gives $\tilde{\lambda}^{0,DT}_{dt\mu}=2.6\times10^6$ s^{-1}. This value agrees well with the rate $\tilde{\lambda}^{0,DT}_{dt\mu}=(1.8\pm0.7)\times10^6$ s^{-1}, determined for a 30-K liquid D-T in the PSI experiment [4]. Note that the formation rate in the solid is somewhat greater than the corresponding rate in the liquid, which is a general law confirmed by experiments. Thus, according to the presented calculation and to the PSI results, $\tilde{\lambda}^0_{dt\mu}\approx\tilde{\lambda}^{0,D_2}_{dt\mu}$. This means that in the steady-state analysis of Ref. [18], a somewhat greater value of $\tilde{\lambda}^{0,D_2}_{dt\mu}$ should have been assumed. In fact, Monte Carlo simulations similar to that performed for gaseous D-T [35] are indispensable for an accurate analysis of such experiments, since several rates change significantly at the lowest energies. Moreover, the thermalization process of muonic atoms in solid hydrogen isotopes is complicated [29,50,51]. It depends on the target temperature, isotopic concentration, and rotational population. The full set of differential cross sections for muonic atom scattering in mixed solid D-T is necessary for the accurate description of μCF in such a target.

V. CONCLUSIONS

A method of calculating the rates of muonic-molecule resonant formation in collision of muonic atoms with condensed hydrogen isotopes has been developed. In the case of polycrystalline hydrogen-isotope targets, detailed calculations have been performed using the Debye model of an isotropic harmonic solid. Values of the resonant-formation rates have been computed for resonant $dt\mu$ formation in frozen D-T and HD targets, at collision energies $\lesssim1$ eV. These rates are very different from those obtained for dilute gaseous hydrogen isotopes and exhibit strong solid-state effects.

At the lowest energies, contributions to the total rate from formation in a rigid lattice and from formation with simultaneous phonon processes can be distinguished. In the high-energy region ($\varepsilon\gtrsim0.1$ eV), for any target, the rate takes a general asymptotic form which depends on the mean kinetic energy of the target molecules. For low-pressure solid and liquid hydrogen isotopes, this energy is much greater than the corresponding energy in a perfect gas. As a result, condensed-matter effects in resonant formation do not disappear even at the highest collision energies. Since the main $dt\mu$ resonances for HD and DT are located far from zero energy, in these cases it is sufficient to use only the asymptotic expression for the formation rate.

The calculated resonance profiles in solids are much broader than in the dilute-gas case. Experimental evidence supporting this conclusion has been found in the time-of-flight measurements of $dt\mu$ resonances at TRIUMF. A quantitative comparison of the theory with these experiments requires, however, complicated Monte Carlo simulations.

The mean values of the $dt\mu$-formation rates for D_2 bound in solid D-T mixtures, averaged over the $t\mu$ kinetic energy under the steady-state conditions, agree well with the PSI and RIKEN-RAL data. Also, the temperature dependence of the mean formation rate determined at RIKEN-RAL for temperatures 5–16 K is revealed by the theory.

ACKNOWLEDGMENTS

We would like to thank Professor K. Nagamine and Professor L. I. Ponomarev for supporting this research and Dr. M. C. Fujiwara and Dr. G. M. Marshall for valuable discussions.

[1] S. S. Gershtein and L. I. Ponomarev, Phys. Lett. **72B**, 80 (1977).
[2] S. E. Jones *et al.*, Phys. Rev. Lett. **56**, 588 (1986).
[3] W. H. Breunlich *et al.*, Phys. Rev. Lett. **58**, 329 (1987).
[4] P. Ackerbauer *et al.*, Nucl. Phys. A **652**, 311 (1999).
[5] W. H. Breunlich, P. Kammel, J. S. Cohen, and M. Leon, Annu. Rev. Nucl. Part. Sci. **39**, 311 (1989).
[6] L. I. Ponomarev, Contemp. Phys. **31**, 219 (1990).
[7] P. Froelich, Adv. Phys. **41**, 405 (1992).
[8] E. A. Vesman, Zh. Eksp. Teor. Fiz. Pis'ma Red. **5**, 113 (1967) [JETP Lett. **5**, 91 (1967)].
[9] Yu. V. Petrov, Phys. Lett. **163B**, 28 (1985).
[10] L. I. Menshikov and L. I. Ponomarev, Phys. Lett. **167B**, 141 (1986).
[11] L. I. Menshikov, Fiz. Elem. Chastits At. Yadra **19**, 1349 (1988) [Sov. J. Part. Nucl. **19**, 583 (1988)].
[12] J. S. Cohen and M. Leon, Phys. Rev. A **39**, 946 (1989).
[13] M. P. Faifman, L. I. Menshikov, and T. A. Strizh, Muon Catal. Fusion **4**, 1 (1989).
[14] M. P. Faifman and L. I. Ponomarev, Phys. Lett. B **265**, 201 (1991).
[15] M. Leon, Phys. Rev. A **49**, 4438 (1994).
[16] Yu. V. Petrov and V. Yu. Petrov, Phys. Lett. B **378**, 1 (1996).
[17] Y. Averin *et al.*, Hyperfine Interact. **138**, 249 (2001).
[18] N. Kawamura *et al.*, Phys. Rev. Lett. **90**, 043401 (2003).
[19] M. C. Fujiwara, Ph.D. thesis, University of British Columbia, 1999.
[20] M. C. Fujiwara *et al.*, Phys. Rev. Lett. **85**, 1642 (2000).
[21] T. A. Porcelli *et al.*, Phys. Rev. Lett. **86**, 3763 (2001).
[22] G. M. Marshall *et al.*, Hyperfine Interact. **138**, 203 (2001).
[23] W. E. Lamb, Phys. Rev. **55**, 190 (1939).
[24] K. S. Singwi and A. Sjölander, Phys. Rev. **120**, 1093 (1960).
[25] L. Van Hove, Phys. Rev. **95**, 249 (1954).
[26] K. Fukushima, Phys. Rev. A **48**, 4130 (1993).
[27] I. F. Silvera, Rev. Mod. Phys. **52**, 393 (1980), and references therein.
[28] P. C. Souers, *Hydrogen Properties for Fusion Energy* (University of California Press, Berkeley, 1986).
[29] A. Adamczak and M. P. Faifman, Phys. Rev. A **64**, 052705 (2001).
[30] P. E. Knowles *et al.*, Phys. Rev. A **56**, 1970 (1997).
[31] L. I. Menshikov, Muon Catal. Fusion **2**, 273 (1988).
[32] C. Petitjean *et al.*, Hyperfine Interact. **118**, 127 (1999).
[33] C. Petitjean, Hyperfine Interact. **138**, 191 (2001).
[34] S. E. Jones, S. E. Anderson, A. J. Caffrey, J. B. Walter, K. D. Watts, J. N. Bradbury, P. A. M. Gram, M. Leon, H. R. Maltrud, and M. A. Paciotti, Phys. Rev. Lett. **51**, 1757 (1983).
[35] M. Jeitler *et al.*, Phys. Rev. A **51**, 2881 (1995).
[36] Yu. V. Petrov and V. Yu. Petrov, Zh. Eksp. Teor. Fiz. **100**, 56 (1991) [Sov. Phys. JETP **73**, 29 (1991)].
[37] V. N. Ostrovski and V. I. Ustimov, Zh. Eksp. Teor. Fiz. **79**, 1228 (1980) [Sov. Phys. JETP **52**, 620 (1980)].
[38] N. T. Padial, J. S. Cohen, and R. B. Walker, Phys. Rev. A **37**, 329 (1988).
[39] Yu. V. Petrov, V. Yu. Petrov, and H. H. Schmidt, Phys. Lett. B **331**, 266 (1994).
[40] A. Akhiezer and I. Pomeranchuk, Zh. Eksp. Teor. Fiz. **17**, 769 (1947) [Zh. Eksp. Teor. Fiz. **11**, 167 (1947)].
[41] G. C. Wick, Phys. Rev. **94**, 1228 (1954).
[42] S. W. Lovesey, *Theory of Neutron Scattering from Condensed Matter* (Clarendon Press, Oxford, 1984).
[43] F. J. Mompeán, M. Garcia-Hernández, F. J. Bermejo, and S. M. Bennington, Phys. Rev. B **54**, 970 (1996).
[44] H. Bethe and G. Placzek, Phys. Rev. **51**, 450 (1937).
[45] M. P. Faifman, T. A. Strizh, E. A. G. Armour, and M. R. Harston, Hyperfine Interact. **101/102**, 179 (1996).
[46] A. Toyoda, K. Ishida, K. Shimomura, S. N. Nakamura, Y. Matsuda, W. Higemoto, T. Matsuzaki, and K. Nagamine, Phys. Rev. Lett. **90**, 243401 (2003).
[47] T. M. Huber *et al.*, Hyperfine Interact. **118**, 159 (1999).
[48] A. Adamczak *et al.*, At. Data Nucl. Data Tables **62**, 255 (1996).
[49] J. S. Cohen, Phys. Rev. A **34**, 2719 (1986).
[50] A. Adamczak, Hyperfine Interact. **119**, 23 (1999).
[51] J. Woźniak *et al.*, Phys. Rev. A **68**, 062502 (2003).